NPL
National Physical Laboratory

Report

NPL REPORT IR 9

Progress in Characterising the Neutron and Gamma Responses of the NPL Liquid Scintillation Spectrometers

N P Hawkes and S F Ashley

NOT RESTRICTED

MAY 2008

National Physical Laboratory | Hampton Road | Teddington | Middlesex | United Kingdom | TW11 0LW

Switchboard 020 8977 3222 | **NPL Helpline** 020 8943 6880 | **Fax** 020 8614 0446 | **www.npl.co.uk**

Department for **Innovation, Universities** & **Skills**

Progress in Characterising the Neutron and Gamma Responses of the NPL Liquid Scintillation Spectrometers

N P Hawkes and S F Ashley
Quality of Life Division

ABSTRACT

The absolute responses of the NPL liquid scintillation spectrometers to monoenergetic neutrons and gammas were measured at various energies in the ranges 1.2 - 17 MeV approximately for neutrons and 0.28 - 1.8 MeV for gammas. Additional measurements of the proton light output function were also carried out. Calculated responses were then obtained for the larger detector using the programs NRESP7 and PHRESP, and compared with the absolute measurements. Finally, response matrices for this detector were generated using responses calculated at closely spaced energies.

ISSN 1754-2952

National Physical Laboratory
Hampton Road, Teddington, Middlesex, TW11 0LW

Approved on behalf of the Managing Director, NPL, by Bajram Zeqiri,
Knowledge Leader, Acoustics & Ionising Radiation Team, authorised
by Martyn Sené, Director, Quality of Life Division

Contents

Figures

Tables

1 Introduction

Neutron spectrometry is important in dosimetry because the quality factor for neutrons changes rapidly with energy in the region from about 1 MeV to a few tens of MeV, so the energy spectrum needs to be known in order to convert fluence into dose.

The organic liquid scintillator NE213, or the equivalent BC501A[1], is a popular choice for neutron spectrometry in this energy region because of its high efficiency and its capacity for high count rates. The scintillator is sensitive to gammas as well as neutrons, but it has the property that the two types of radiation generate scintillations with slightly different time profiles, allowing them to be distinguished by pulse shape discrimination (PSD) implemented by suitable electronics.

In 1991, NPL acquired a pair of NE213 neutron spectrometers designed, built and characterised by Green *et al.*[2]. The larger one (referred to as the 'Large' spectrometer) had a scintillator volume 60 mm diameter by 60 mm long, while the 'Small' spectrometer was 20 mm by 20 mm. The scintillator cells were constructed to an in-house design in which the expansion bubble in the scintillator cell (a necessary feature with NE213 because of its high thermal expansion coefficient) was confined to a chamber at the end of the cell furthest from the photomultiplier.

PSD was achieved by the Owen technique[3], in which the last dynode of the photomultiplier is deliberately driven into space charge saturation. The duration of this saturation, and hence the amplitude of the pulse from the dynode, depends on the original pulse shape, and is therefore different for neutron and gamma events of the same light output. An earlier dynode provides an undistorted signal proportional to light output. The two signals are captured in coincidence by a two-parameter data acquisition system, and the neutron and gamma events form two distinct ridges in the parameter space. At NPL the 2-parameter display is conventionally set up with 'Shape' on the *Y*-axis and 'Energy' (properly 'Light output') on the *X*-axis. The Owen technique has the advantage that the PSD is done by the photomultiplier's own dynodes, and no specialised shape-sensitive electronics is needed (Figure 1).

Green *et al.* tested and characterised these spectrometers extensively. In particular they provided neutron response matrices to allow the incident neutron spectrum to be unfolded from the measured pulse height spectrum using unfolding codes such as RADAK[4]. These matrices were generated by calculating the detector response at closely spaced energies using the program O5S[5], and then assembling the calculated responses into a matrix in a suitable format for the unfolding program. Green *et al.* validated O5S for this application by measuring the detector response absolutely at several selected neutron energies and then comparing these measurements with the corresponding O5S calculations. The measurements were carried out at the monoenergetic irradiation facilities of NPL, Harwell and Birmingham University.

The spectrometers were incorporated into NPL's suite of instruments and put into routine use. By 2003, however, it had become apparent that their performance was declining. Table 1 shows how the resolution of the 1062 keV Compton edge from ^{22}Na had broadened with time.

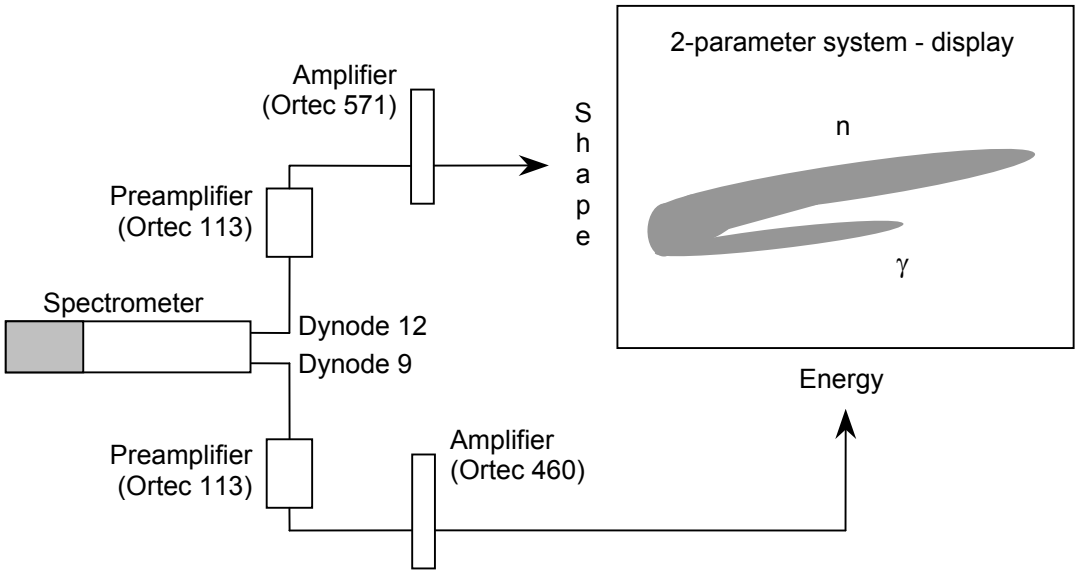

Figure 1. Data acquisition system used with the NPL NE213 spectrometers (schematic).

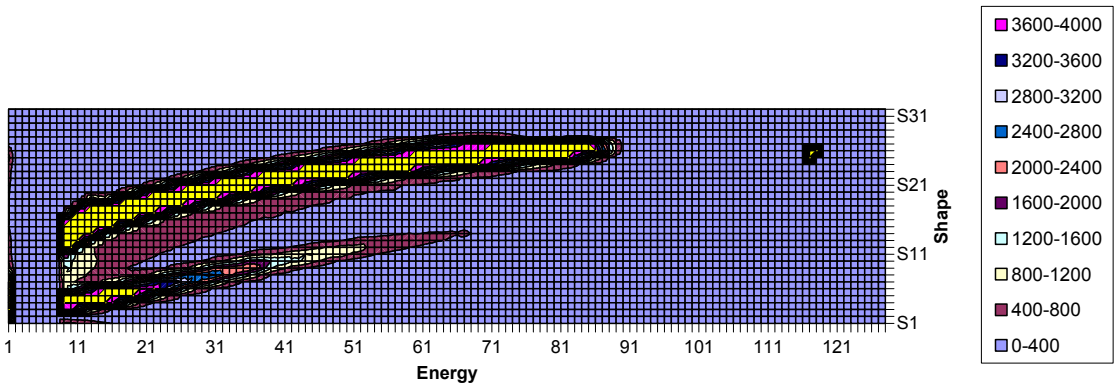

Figure 2. A typical actual 2-parameter histogram corresponding to the above schematic. (The bright yellow colouration denotes cells with more than 4000 counts.)

Table 1. Variation of ^{22}Na resolution with time.

	Original value (c. 1990)	2003 value	Value with new cell
Large NE213	12 %	24 %	13 %
Small NE213	9½ %	16 %	10½ %

The figures in each case are calculated from the formula

$$\text{Resolution (\%)} = \frac{100\,(C_{12.5} - C_{87.5})}{C_{50}} \qquad (1)$$

where C_p is the spectrum channel number (counting from the channel that corresponds to zero light output) at which the counts-per-channel figure is p% of the maximum at the edge.

Inspection of the scintillator cells raised suspicions about the condition of the scintillator. NE213 is normally a clear liquid (with perhaps a hint of blue under some lighting conditions), but the liquid in the cells was pale green. Furthermore, a large number of blister-like raised areas could be seen in the reflective paint on the inner surface of the cells. These effects are not known to be problems with NE213[6], even in cells as old as those here, and they remain unexplained. Nevertheless, the scintillator was clearly implicated, and the decision was taken to replace the cells with new ones of the same size and shape containing BC501A.

The cell design chosen was the MAB-1 type[1], in which the expansion bubble is confined to a coiled tube within the hollow curved side wall of the cylindrical chamber. The casings of the original spectrometers were modified to allow the new cells to be attached, but no other alterations were made. In particular, the Owen PSD system was retained. The new cell design meant that the favoured orientation for irradiations was now end-on instead of side-on as previously.

When the ^{22}Na resolutions were re-measured, the results were as shown in the final column of Table 1. The new resolution figures were greatly improved, being nearly restored to the 1990 values, and the scintillator replacement was deemed successful. However, with such a large change to the spectrometers, it was felt necessary to re-characterise them.

Such work requires significant effort, as detailed in this report, but also afforded the opportunity to update the neutron response matrices using the more up-to-date programs now available for calculating neutron responses. Furthermore, with the availability of similar programs for gammas, additional matrices could be produced to allow gamma spectra to be unfolded. Hitherto gamma data had simply been discarded, but now, provided that neutron and gamma pulse height spectra could be extracted reliably by placing a dividing line between the two ridges of Figure 2, both spectra could be measured simultaneously with the same instrument. This is a useful ability when neutron fields are always accompanied by gammas. The resolution of organic scintillators is poor compared with, say, high purity germanium, but in many applications the speed and convenience of a simultaneous measurement would outweigh this.

2 Scope of the present work

As described in Section 1, the aim of the present work was to produce updated neutron response matrices, and to produce gamma response matrices for the first time, for the NPL NE213 spectrometers.

In common with the original Green *et al.* work, the response matrices were derived by calculation, because it is not practical to make individual measurements at the large number of closely spaced energies needed to generate a response matrix. Monoenergetic fields may in any case not be available at the required energies. The programs used for the calculation were first validated experimentally by making absolute measurements (i.e. with a known fluence of neutrons or gammas striking the detector) at selected energies, and comparing the results with corresponding calculations.

The program used for calculating gamma responses was PHRESP[7], and that for neutron responses was NRESP7[8]. The response matrices were constructed in a format suitable for use with the unfolding code GRAVELW, which is part of the HEPROW[9] package. All these programs originate from the Physikalisch-Technische Bundesanstalt (PTB) in Germany.

This report describes the experimental measurements for both of the NPL NE213 spectrometers. For the Large spectrometer, the data analysis and the response matrix calculations are also described. The corresponding analysis and calculation for the Small spectrometer will be described in a later report.

3 Light Output Units

The light produced by electrons is commonly regarded as linear with energy (with a small offset), provided the energy is above about 40 keV[10]. (Some authors[11] report that the output becomes non-linear again above 1.6 MeV.) Assuming the linear relationship holds, the light output L in "light output units" (LU) is therefore related to the electron energy E in MeV by

$$L = c\,(E - E_0) \qquad (2)$$

where c is a constant. Reported values of E_0 differ between authors, but are commonly in the region of 0.005 - 0.015 MeV[11, 12]. The PTB convention for light output units, which will be adopted here as well, is to set c = 1 LU / MeV and to define 1 LU as the light produced by an electron of energy (1 + E_0) MeV.

An additional convention adopted in the present work is that the bins in pulse height spectra are labelled with the light output at the centre of the bin.

4 Measurements

4.1 Gamma measurements

A selection of gamma-ray sources were used to measure responses over as wide an energy range as possible, to calibrate the analysis system in terms of light output, and to obtain experimental spectra with which to validate the calculations.

Table 2. Gamma-ray sources used in the measurements.

Nuclide	Gamma energy, MeV	Compton energy, MeV
^{24}Na	2.754	2.520
"	1.369	1.154
^{88}Y	1.836	1.612
"	0.898	0.699
^{60}Co	1.333	1.118
"	1.173	0.963
^{22}Na	1.275	1.062
"	0.511	0.341
^{54}Mn	0.835	0.639
^{137}Cs	0.662	0.477
^{203}Hg	0.279	0.146

Most of the sources were disc-type Isotrak point sources supplied by High Tech Sources Ltd.[13] These consist of a 1 mm ion exchange bead at the centre of a plastic disc 3 mm thick and 25 mm diameter. The ^{24}Na source was an exception. It has a half life of only 15 hours, and is not available commercially. Instead, it was prepared by the NPL Radioactivity Group, from material activated at the Consort reactor[14] in Ascot. A few drops of active solution were placed at the centre of a thin circular plastic film (supported at the periphery by an aluminium ring) and allowed to evaporate to dryness, producing an active area a few millimetres in diameter.

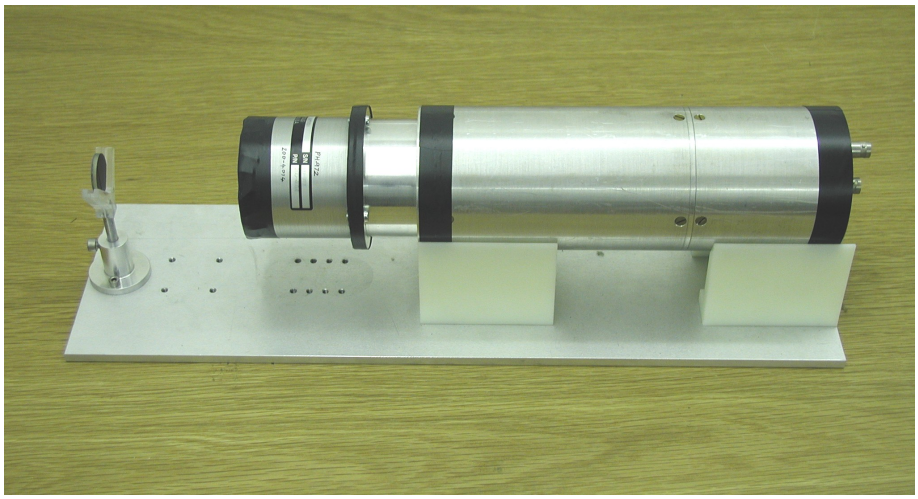

Figure 3. Large spectrometer mounted on the gamma measurement jig.

The nominal activity of the commercial sources was 370 kBq, but each was additionally accompanied by a certificate from the manufacturer stating the measured activity at a given reference date.

To carry out the measurements, the source and the spectrometer were mounted on a custom built jig (Figure 3), which positioned the source on the spectrometer axis and at a well determined distance from the front face. The distance was chosen to keep the dead time of the system below about 10%, and was 9.65 or 9.75 cm for the Large spectrometer and 4.15 cm for the Small.

With such a wide range of energies to be covered, the gain of the Energy amplifier had to be changed several times during the measurements, and so a precision pulser was used to establish the gain ratio between different runs and allow them all to be placed on a common scale. The same pulser was also used to establish the spectrum channel corresponding to zero light output in each run.

Due to the proximity of the source to the spectrometer, background was neglected in making the measurements.

4.2 Neutron measurements

Neutron measurements were carried out with monoenergetic neutrons at 1.2, 2.5 and 5.0 MeV, produced by directing proton or deuteron beams from the NPL Van de Graaff accelerator onto a suitable neutron-producing target. In addition, the spectrometers were taken to the neutron facility at PTB, where high energy neutrons are available. This allowed monoenergetic measurements to be made at energies of 16 and 17 MeV (Large spectrometer) and at 15.5 MeV (Small).

In each case the spectrometer was placed near the centre of the facility's low-scatter area at a known distance of about 1.5 m from the target. A shadow cone measurement was carried out at each energy to allow the room scatter component to be subtracted from the 'total' measurement made without the cone.

At NPL, the neutron fluence delivered to the spectrometer was determined by calibrating the beam current integrator, which measures the total beam charge incident on the target, in terms of the neutron fluence (at a known position) per unit of charge. This was done using the NPL long counter, the efficiency of which is well determined, in a calibration run at the start of each day of measurement. The current integrator was also used to normalise the shadow cone run to the same target yield as the 'total' run.

At PTB, the measurements were carried out at the same time as an international comparison of neutron fluence monitors, and therefore PTB could not provide their value for the fluence delivered to the instrument as they normally would. However, the NPL dePangher long counter was part of the intercomparison, and so the value from that was used to calibrate the PTB neutron monitor for each day. As at NPL, the current integrator was used to relate the shadow cone run to the total run.

It is desirable to have neutron data at a large number of energies in order to establish the scintillator's light output for protons as a function of proton energy. Absolute measurements, in which the neutron fluence is known, are time consuming, and generally only one neutron energy can be set up and used per day. Determining the proton light output this way would be slow and expensive. However, it is not necessary to know the delivered fluence; all that is needed is the position of the upper edge of the pulse height distribution. Similarly, the room scatter need not be known, as it is expected to affect only the low energy part of the spectrum. A separate set of

measurements was therefore carried out at NPL, omitting the long counter calibrations and shadow cone measurements but covering 14 neutron energies from 0.6 to 6.4 MeV in one 8-hour day (once set up).

In all cases, at least one measurement with a ^{22}Na gamma source was made during each day in order to establish the energy calibration. The precision pulser was used as before to relate runs at different gains and to establish the channel number corresponding to zero light output.

5 Analysis and Calculation

5.1 Gamma spectra

5.1.1 Electron light output

The first stage in the calculation of the gamma spectra is to establish the parameters of the light output function for electrons.

For gamma rays striking an organic scintillator, the predominant interaction mechanism is Compton scattering from an electron. This produces a spread of electron energies up to a sharp cutoff at the Compton energy E_c, a quantity that is related to the gamma-ray energy E_γ by

$$E_c = \frac{E_\gamma}{1 + \frac{m_e c^2}{2E_\gamma}}$$

where $m_e c^2$ is the rest energy of the electron (0.511 MeV). Measurements with suitably selected sources therefore produce a set of relatively sharp Compton edges at the corresponding value of E_c, and by measuring the light output at the these edges the relationship between electron energy and light output can be established.

However, the observed Compton edge does not correspond exactly to the true position of the edge, because of the effect of detector resolution.

Figure 4 shows a typical Compton distribution, with no added resolution (black curve) and also with successively larger Gaussian smearing folded in. (For each smeared curve in the Figure, the standard deviation of the Gaussian is constant, and equal to the stated percentage of the true Compton light output.) The filled circles show the half-height positions of each smeared edge, and it is clear that these positions are displaced increasingly above the true position as the smearing is increased.

As was pointed out by Dietze[15] and by Dietze and Klein[10], the extent of the displacement will depend on the original shape of the unsmeared Compton distribution, and therefore on the gamma ray energy and the size and shape of the scintillator, as well as the extent of the smearing. For a correct calibration, the displacement factor (the ratio of the Compton edge's half-height position to the true Compton position) must be known for each gamma-ray energy and for the particular spectrometer in question.

This can be done with the help of a program such as PHRESP that calculates gamma pulse height spectra in organic liquid scintillators. The following procedure will give the required factor for a particular gamma energy:

1. Calculate the resolution-free Compton distribution for the gamma energy and scintillator cell in question.
2. Apply Gaussian smearing at a range of different smearing values.
3. For each smeared curve, measure the displacement factor. Also measure the percentage 7/8 – to – 1/8 width as defined in Equation 1 on page 3.
4. From the data obtained from the smeared curves, plot a chart of displacement factor *vs.* 7/8 – to – 1/8 percentage width.
5. Measure the 7/8 – to – 1/8 percentage width of the experimental pulse height spectrum, and read off the displacement factor from the chart.

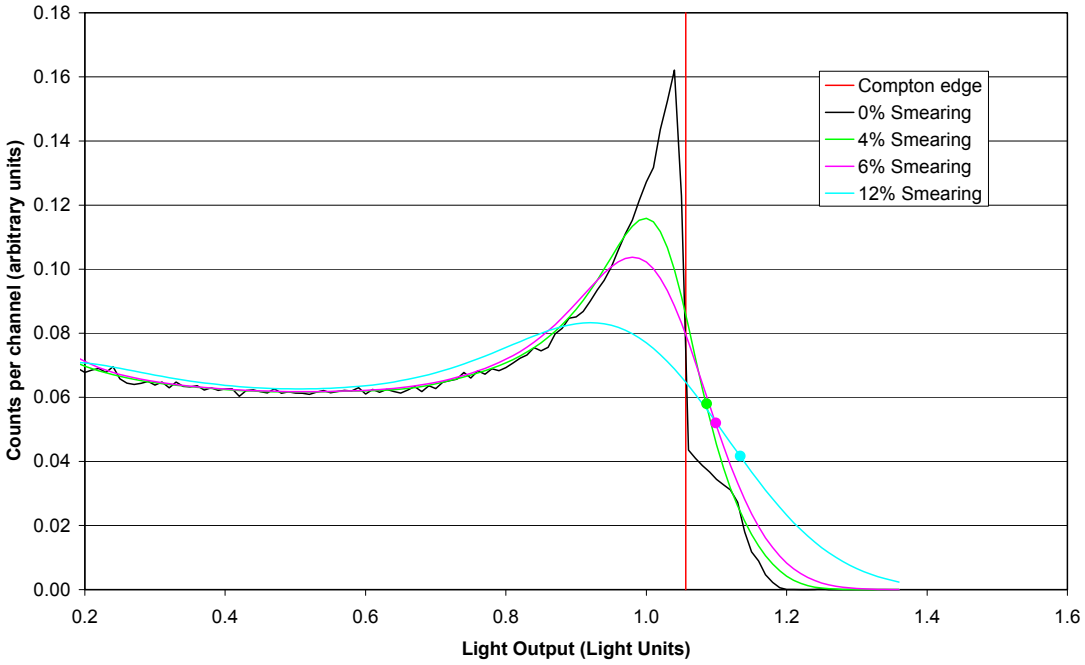

Figure 4. Displacement of the apparent Compton position with resolution. The filled circles show the half-height positions for each smeared edge, and the progressive displacement away from the true Compton position is evident. (The shoulder above the sharp edge on the 0% spectrum is due to multiple scattering.)

An element of iteration has to be used here, as the electron light output is needed for the calculation in step (1), but the displacement factors required to derive it have not yet been determined. The solution is to adopt a temporary estimated light output function for step (1), and in the present work the default function provided with PHRESP (and found by PTB to be suitable for their detectors) was used for this. When all the factors are available, a new function is derived from the experimental data, and substituted into the program for all subsequent calculations.

At steps (3) and (4) it is also useful to plot a graph of the Gaussian smearing width *vs.* 7/8 – to – 1/8 percentage width, so that at step (5) the true detector resolution (i.e. the underlying Gaussian smearing rather than the effect that such smearing has on the Compton edge) can be determined for each experimental spectrum. This is important because the detector resolution varies with light output, and the correct light-dependent smearing must be folded into the calculated spectra for comparison with experiment. This contrasts with what has been done in the analysis so far, namely smearing the spectra using a fixed value for the smearing, an approximation that has been necessary because the light dependence is not yet known. (In any case, we have only been interested in the effects of smearing over the narrow region of the Compton edge.) A further reason for deriving the variation of smearing with light output is that this variation is expected to follow a certain form based on the origin of the noise components, and it is useful to check that this is indeed observed (see Figure 9 later in this section).

In the present work, the procedure outlined above was followed for all source spectra except ^{24}Na (which was omitted from the calibration and used as test of the unfolding procedure instead) and ^{60}Co. The two principal gamma lines from the latter source are close enough in energy for their Compton edges to overlap at the resolution of the

spectrometer in question, and the procedure did not produce a satisfactory result; a different technique was used instead, and this is described below.

Figure 5 and Figure 6 show the charts derived at step (4) for the Large spectrometer. Note that Figure 6 refers to smearing FWHM rather than standard deviation as in Figure 4.

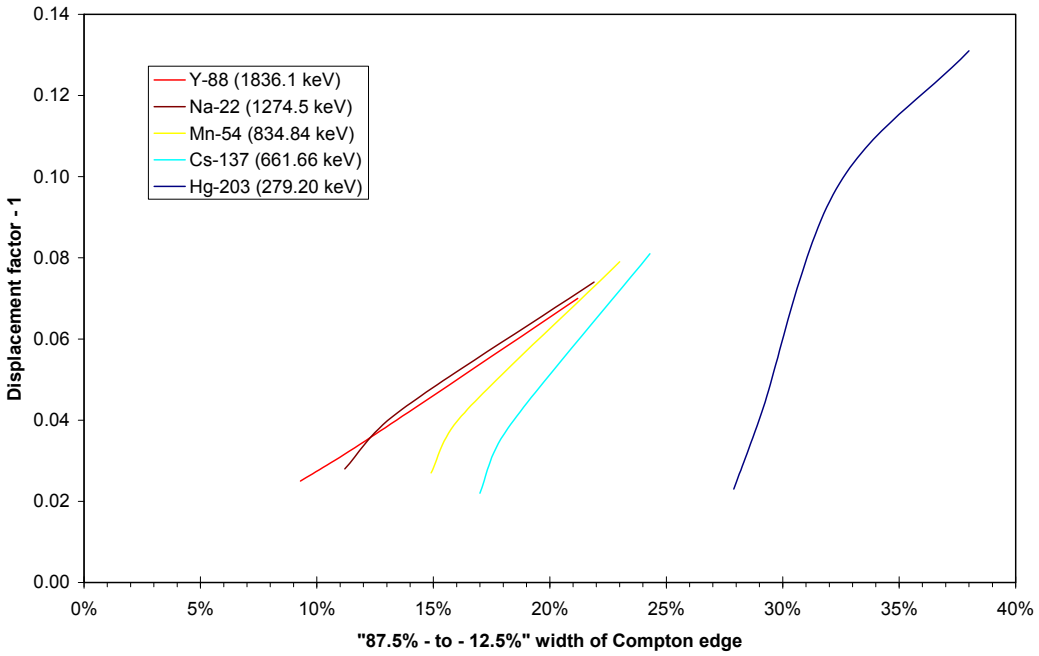

Figure 5. Chart of calculated displacement factor vs. calculated Compton edge width for calibration sources and the Large spectrometer.

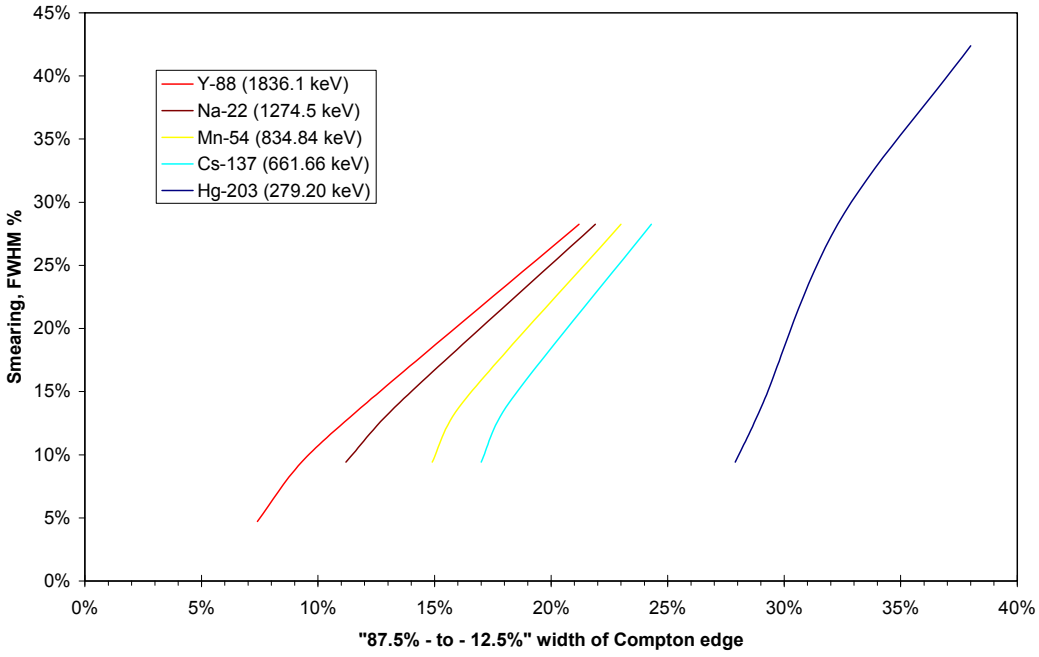

Figure 6. Chart of calculated smearing FWHM vs. calculated width of Compton edge for calibration sources and the Large spectrometer.

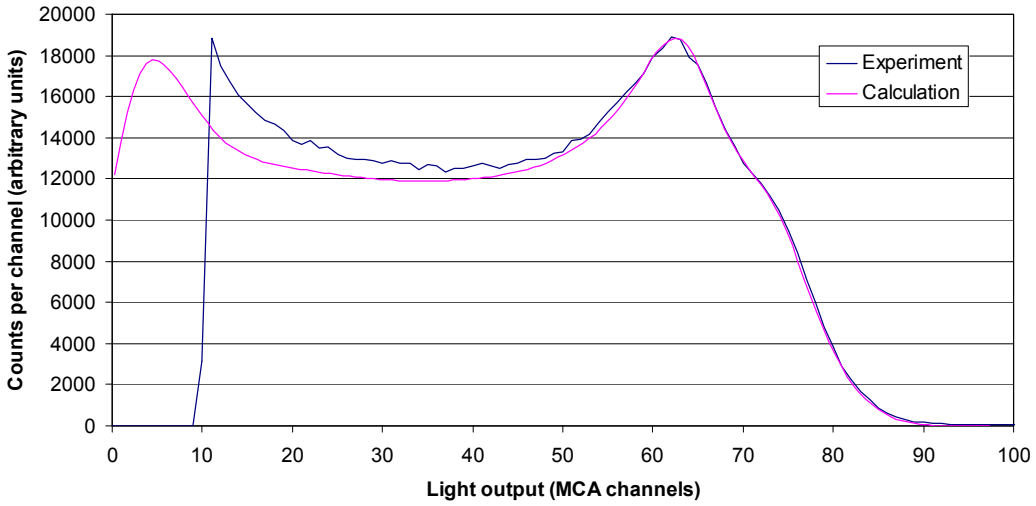

Figure 7. Light output calibration for ^{60}Co in the Large spectrometer.

^{60}Co was treated differently because the procedure described above proved unsuitable for overlapping Compton edges. Instead, an Excel spreadsheet was set up containing the two unsmeared Compton distributions, and then a separate adjustable smearing (not varied with light output) was applied to each and the two added together. The horizontal and vertical scales were also adjustable, and a satisfactory match to the experimental spectrum over the region of the Compton edge (which is all that is required at this stage) was sought. On achieving this (Figure 7), the following were then known:

- the smearing widths (spectrometer resolutions) at the two individual Compton edges;
- the displacement factors relative to the half-height of the single edge in the experimental spectrum.

Table 3 shows the displacement factors and underlying spectrometer resolutions deduced for the Large spectrometer at the calibration energies. Figure 8 shows the electron light calibration that follows from this, and Figure 9 shows how the spectrometer resolution varies with light output.

Table 3. Displacement factors and resolutions deduced for the Large spectrometer.

Nuclide	Gamma energy, MeV	Compton energy, MeV	Observed 7/8 – 1/8 width, %	Displace-ment factor	Spectrometer resolution, FWHM %
Y-88	1.836	1.612	9.3	1.025	9.4
Co-60 (high)	1.333	1.119		0.989	10.4
Na-22	1.275	1.062	11.2	1.030	10.2
Co-60 (low)	1.173	0.963		1.146	10.4
Mn-54	0.835	0.639	15.2	1.032	11.1
Cs-137	0.662	0.477	17.4	1.029	11.4
Hg-203	0.279	0.146	36.6	1.123	39.0

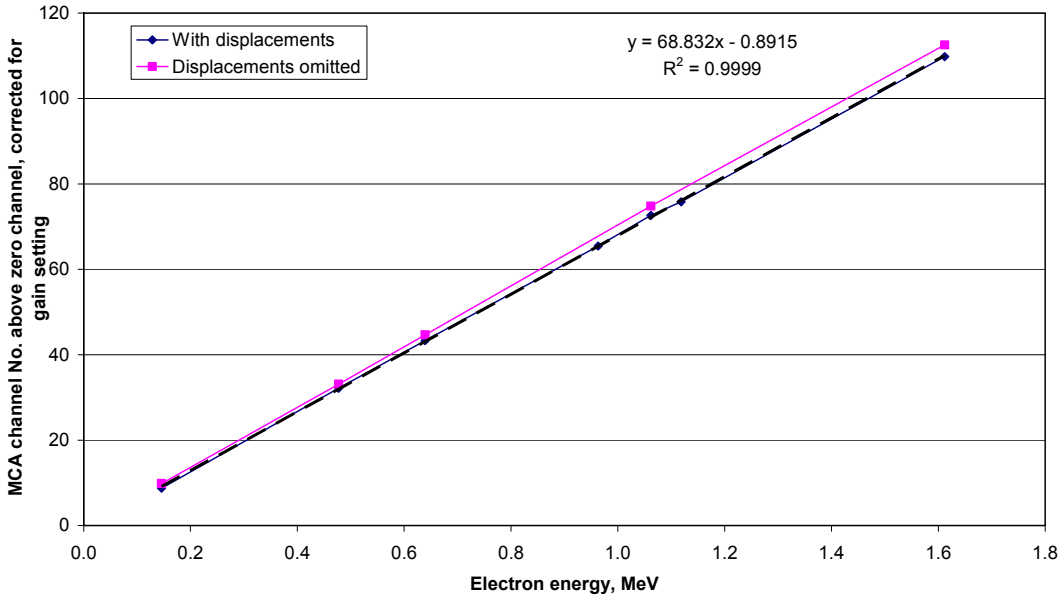

Figure 8. Electron light calibration for the Large spectrometer.

In Figure 8, the deduced displacement factors are finally brought together with the observed positions of the Compton edges to give the calibration of the multichannel analyser (MCA) in terms of electron light output (blue curve). The dotted line is a linear fit to the data points, and confirms that the electron light output can be regarded as linear over the range studied. The parameters of the fit show zero light output for an electron energy of 0.013 MeV, i.e. that the constant E_0 in the electron light output function (Equation (2) on page 4) is equal to 0.013 MeV for the Large spectrometer.

The purple curve in the Figure shows the calibration that would have been deduced if the displacement factors had not been included.

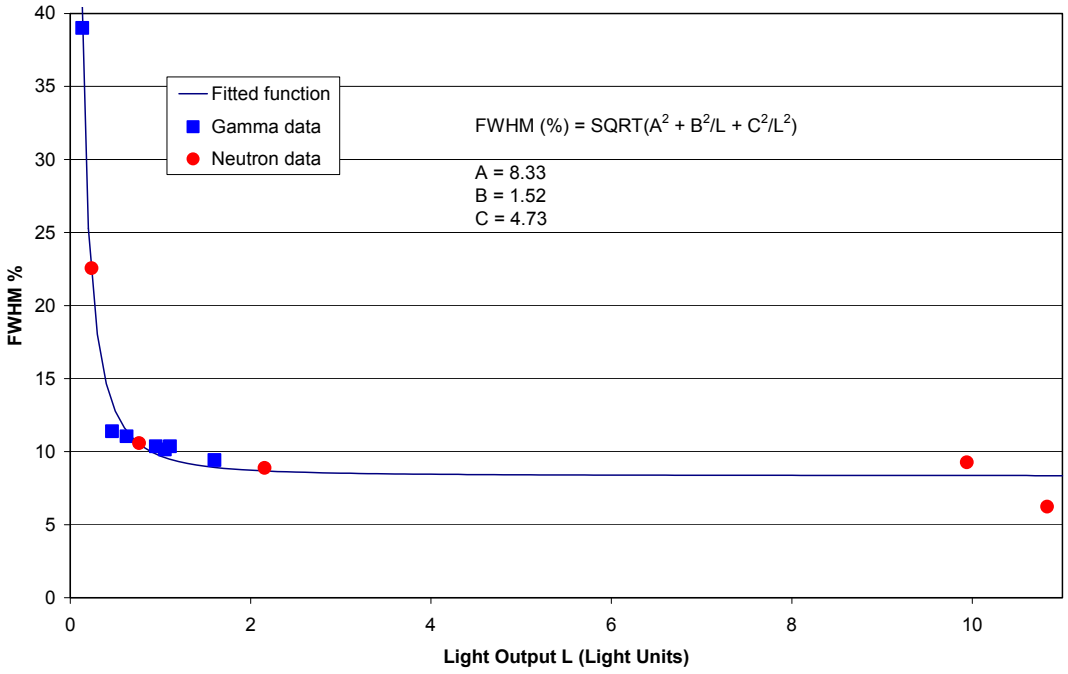

Figure 9. Light output resolution vs. light output for the Large spectrometer.

In Figure 9, the spectrometer resolution (expressed as the percentage FWHM of the underlying Gaussian smearing) is plotted as a function of light output. There are expected to be three different contributions to the resolution so expressed, each with a different dependence on the light output $L^{(10)}$:

- a constant term, from the position-dependent transmission efficiency of light from the scintillator to the photomultiplier;
- a term in $1/L^{0.5}$, due to photon and electron statistics;
- a term in $1/L$, due to electronic noise.

The Figure shows that a function consisting of these contributions added in quadrature can be fitted to the data satisfactorily. Furthermore, the neutron data (to be described in Section 5.2.1) and the gamma data can be fitted by the same parameters. This shows that the spectrometer resolution depends only on the light from an event, and not on the reaction that caused it.

5.1.2 Calculated gamma pulse height spectra

With the electron light output function and the resolution function now known, and the relationship between MCA channels and light output established, the program PHRESP could now be validated for this application by calculating the pulse height spectra corresponding to the experimental gamma source measurements made earlier.

Figure 10 - Figure 15 below show these comparisons for each of the gamma sources. In each case, the vertical axis is in counts per unit fluence of the stated gamma ray at the spectrometer face, divided by the bin width in light units. Where the source produces more than one gamma line, the calculated components have been added in the proportion given in the manufacturer's data sheet that accompanied the source. The decay of the source since the calibration date was included in the calculation.

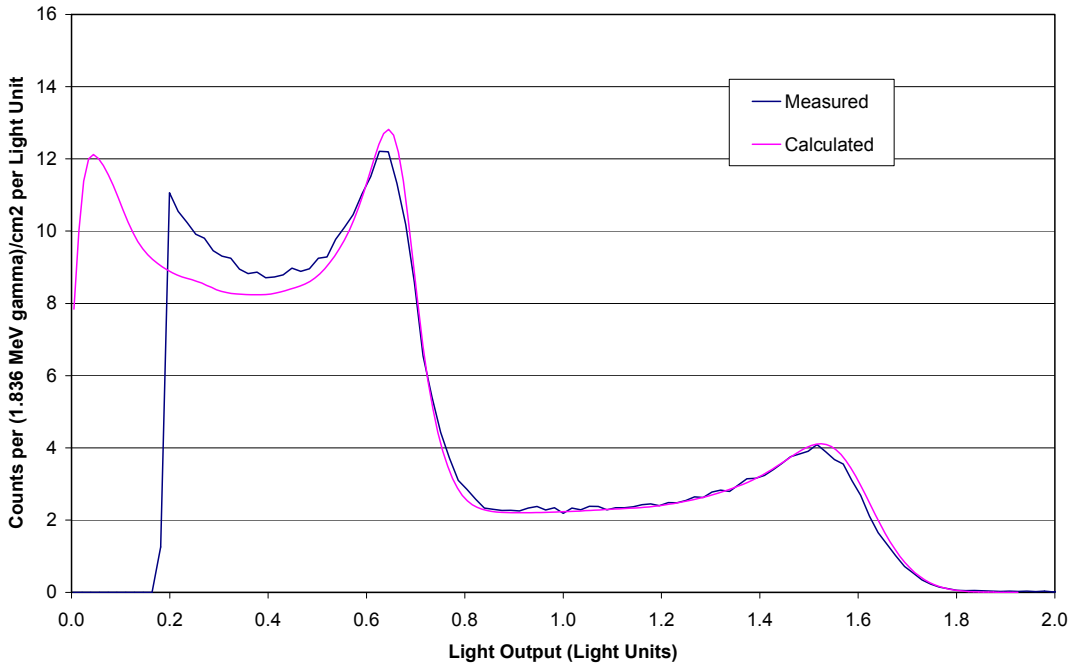

Figure 10. ^{88}Y pulse height spectrum, measured and calculated.

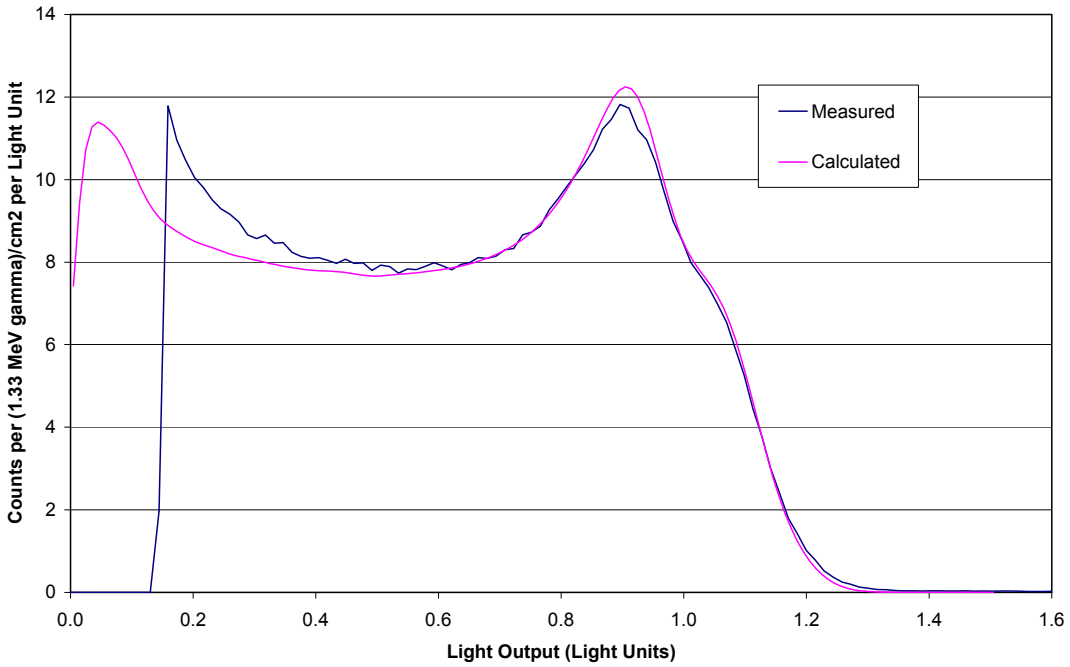

Figure 11. ^{60}Co pulse height spectrum, measured and calculated

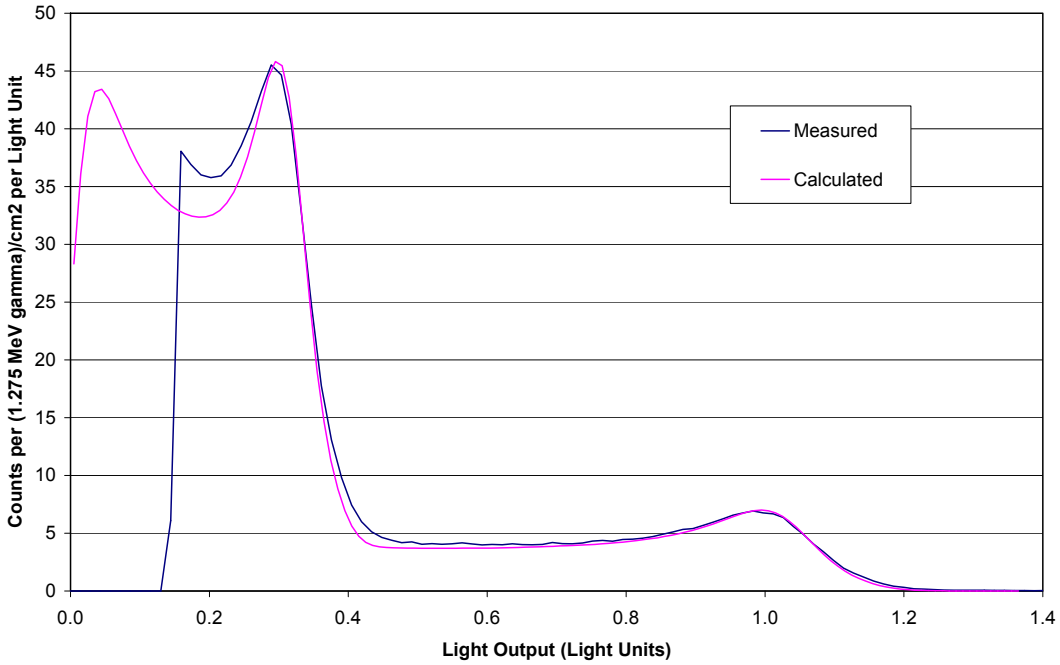

Figure 12. ^{22}Na pulse height spectrum, measured and calculated

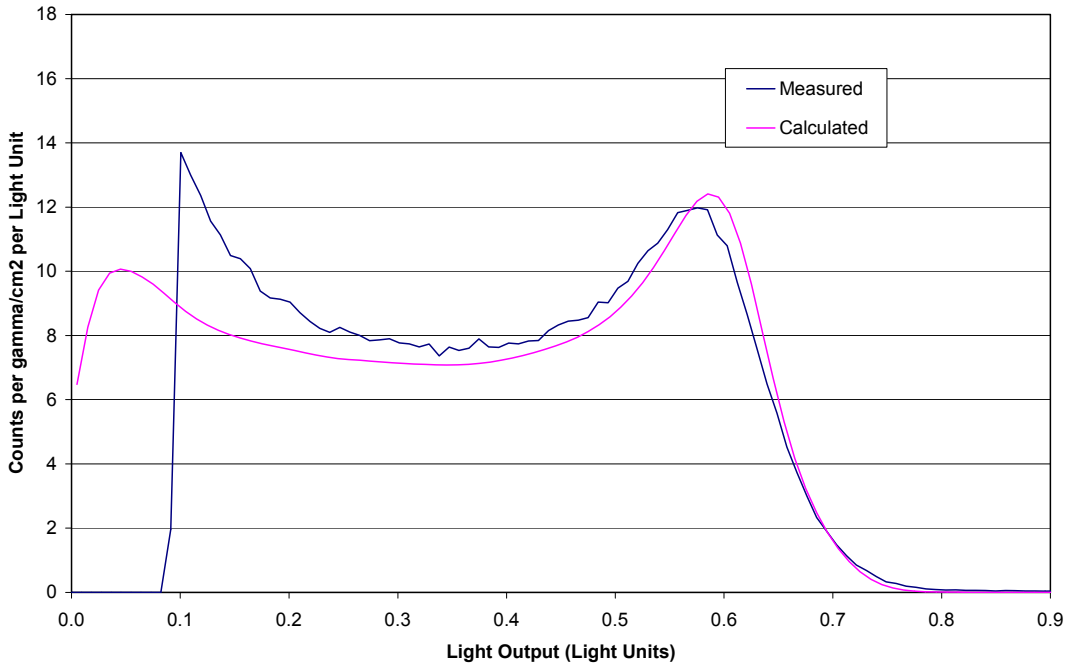

Figure 13. ^{54}Mn pulse height spectrum, measured and calculated.

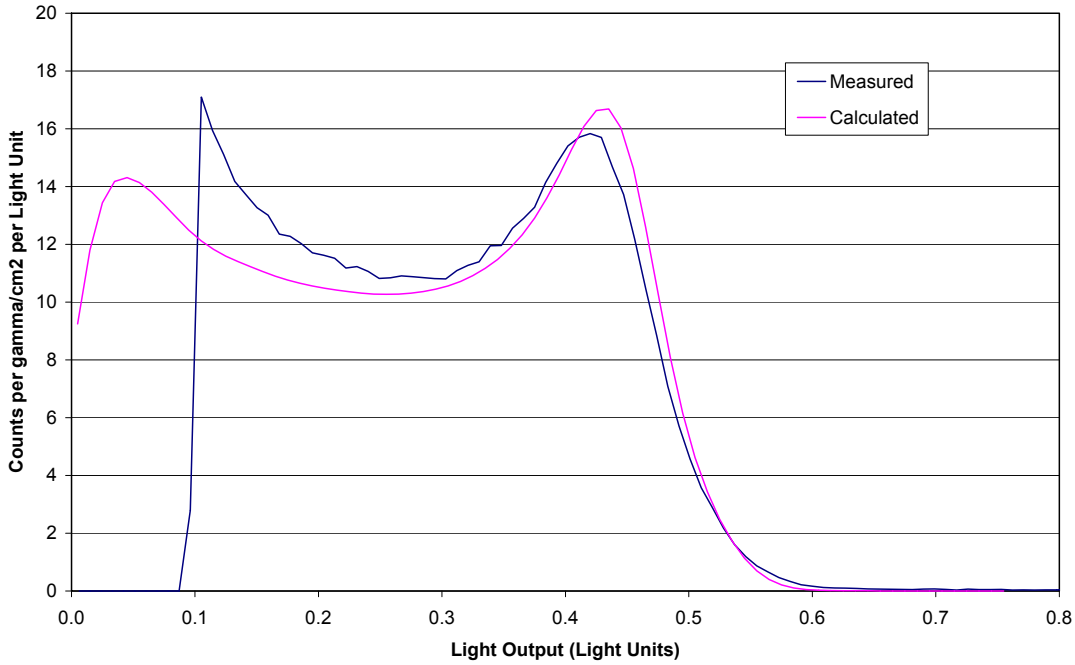

Figure 14. ^{137}Cs pulse height spectrum, measured and calculated.

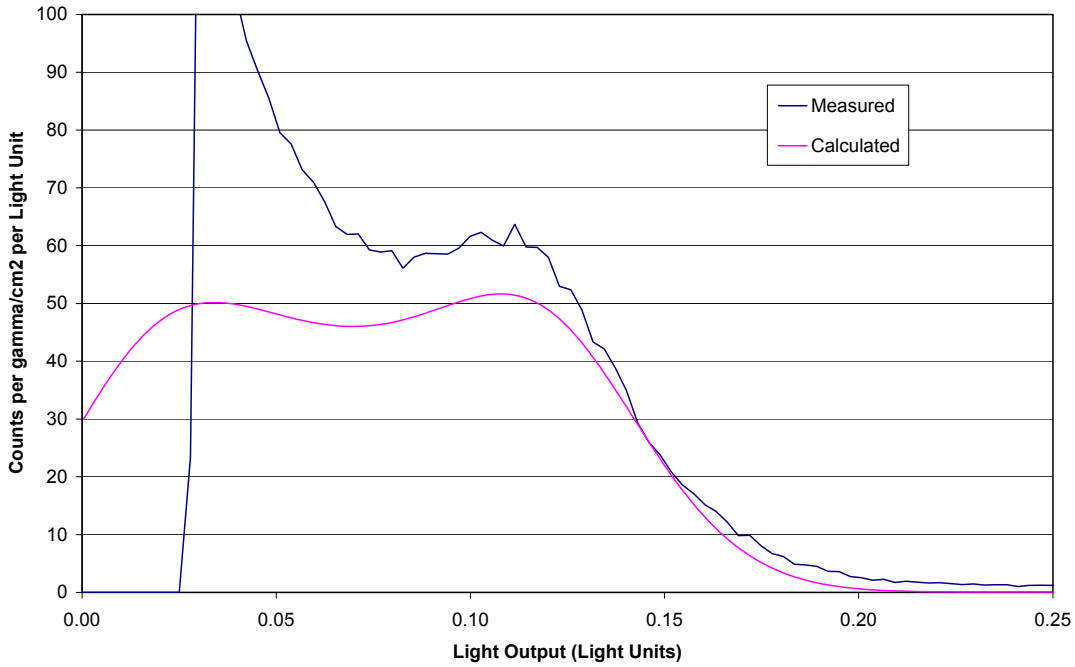

Figure 15. ^{203}Hg pulse height spectrum, measured and calculated.

In all cases, both horizontal and vertical scales are absolute, except in so far as the gamma line (or higher energy gamma line where the source has two) has contributed to the light output determination. The lower energy gamma, where there is one, was not used in this determination, and represents a completely independent test of the calculation.

The match between measurement and calculation is generally reasonable to good, especially at the higher gamma energies and at the high light output end of the responses. Most of the spectra show a discrepancy just above the experimental threshold, the spectrometer having an excess of counts over the calculation, and for the lowest energy gamma spectra this discrepancy extends over most of the spectrum. This is presumably due to processes not modelled in the calculation, such as pile-up of small pulses.

Overall, the match was considered good enough to proceed to a response matrix calculation.

5.1.3 Response matrix calculations

To generate a response matrix, a large number of response calculations are carried out at closely spaced energies, and the resulting spectra are assembled in the format appropriate for the unfolding program to be used.

To determine the energies at which to calculate the responses, the approach of the utility programs provided with PHRESP for this purpose was adopted. This approach is based on the principle that response functions are to be spaced most closely where the spectrometer resolution ΔL is smallest, and more widely where ΔL is larger. Roughly speaking, the method maintains the same number (7 in the present case) of response functions per light increment $\Delta L(L)$, where $\Delta L(L)$ is the absolute FWHM as derived from the formula in Figure 9, i.e., $\Delta L(L) = (A^2L^2 + B^2L + C^2)^{0.5}$ / 100 Light Units. For the Large spectrometer, a total of 232 response functions were calculated, covering

gamma energies from 66.4 keV to 4930.3 keV, at intervals ranging from 6.8 keV to 58.4 keV.

For these calculations, the geometry of the model was altered to have a parallel gamma beam instead of a point source, as the distance to the source will not in general be known.

The calculated responses were assembled into a HEPROW-format response matrix using the utility programs BMATASC (which assembles a matrix with unsmeared response functions) and RSPGW (which adds smearing). These programs are part of the PHRESP and HEPROW packages.

5.1.4 Trial unfolding of a spectrum

To test the new response matrix, the experimental ^{24}Na pulse height spectrum was unfolded using the HEPROW program GRAVELW.

The experimental pulse height spectrum recorded over a 20 minute counting interval, with NPL source No. S05057 at 9.75 cm from the front face of the spectrometer, is shown in Figure 16.

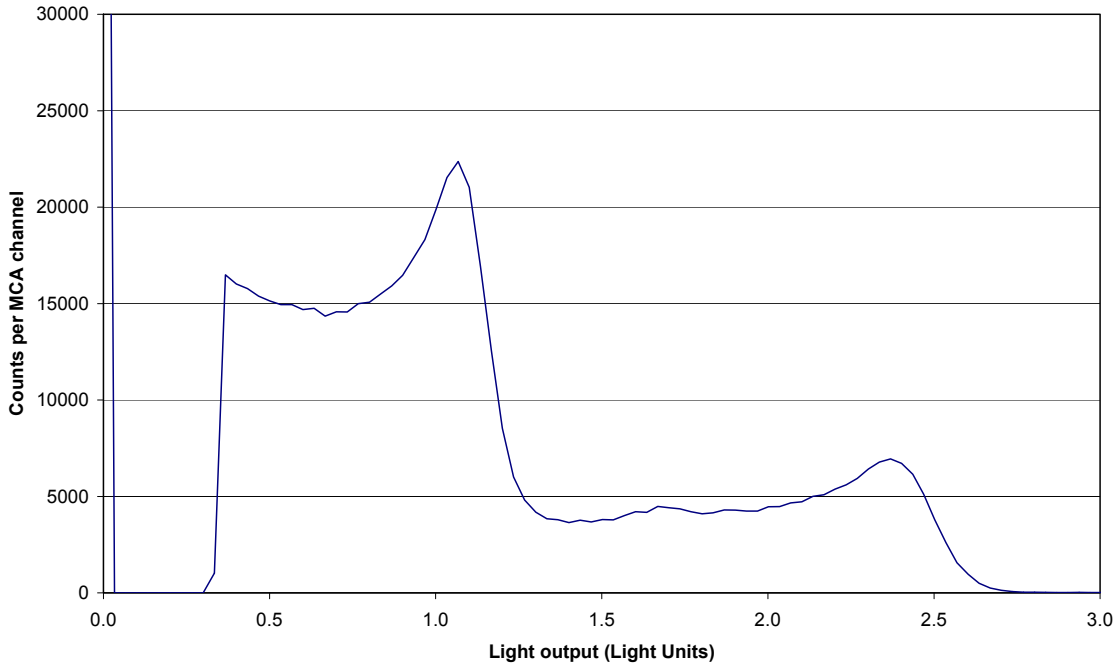

Figure 16. Pulse height spectrum from the ^{24}Na source.

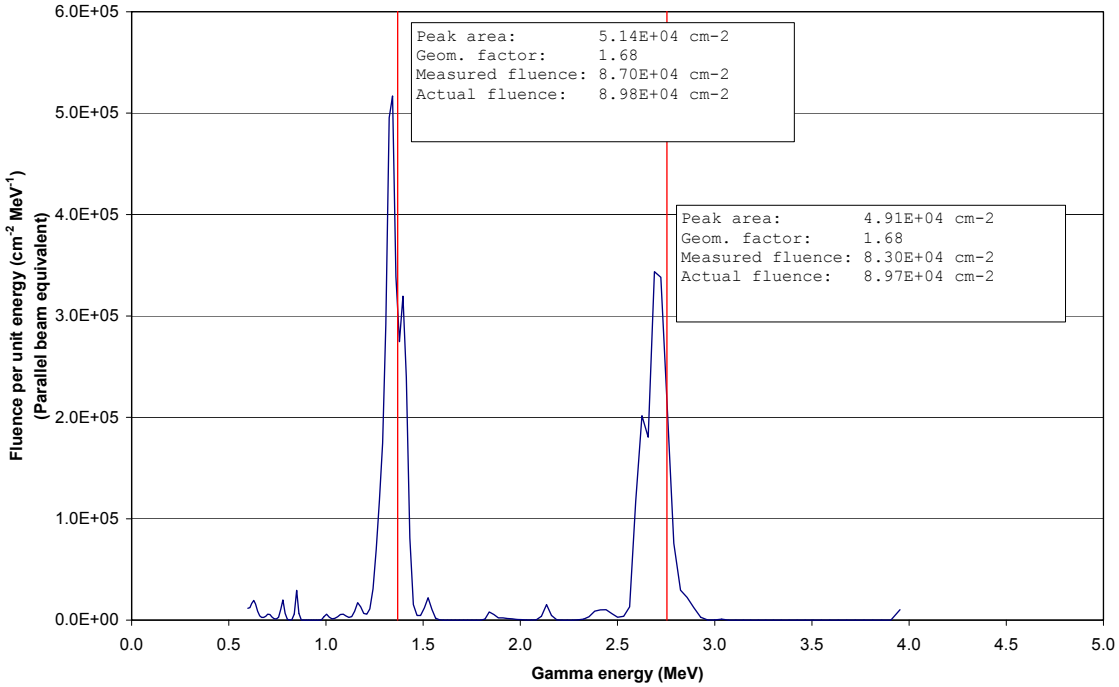

Figure 17. Gamma energy spectrum unfolded by GRAVELW.

The spectrum file from the MCA was converted to HEPROW format and passed to GRAVELW for unfolding, and the result is shown in Figure 17.

The red lines show the expected positions of the two gamma components, and these have been reproduced well by the unfolding (especially the lower component). The unfolded widths are surprisingly large, however.

The areas of the peaks give the associated fluence in terms of a parallel gamma beam (because this is how the response functions were calculated). For comparison with the actual fluence from the point source, PHRESP was used to calculate a geometry correction factor, converting the 'parallel' fluence into the equivalent fluence, at the centre of the detector face, from a point source at the source location. The results are set out in the Figure, and the actual fluence at the centre of the detector face (calculated from the known activity of the source) has been reproduced well by the unfolding process.

PHRESP calculations will not usually be available for interpreting general measurements made with the spectrometer. However, in the present case at least, a good approximation to the correct value would have been obtained by simply assuming that the fluence deduced from the unfolding applied at the centre of the scintillator.

5.2 Neutron spectra

5.2.1 Proton light output

As with the gamma data, the first step is to establish the applicable light output function.

The main interaction mechanism for neutrons striking an organic scintillator is elastic scattering from a proton. For monoenergetic neutrons, and if multiple scattering is neglected, this results in a rectangular distribution of proton energies from zero up to the energy of the neutrons. Hence the upper edge of this recoil distribution corresponds to protons having the same energy as the neutrons.

Factors such as multiple scattering, and non-linearity of the proton light output, distort the pulse height spectrum away from the basic rectangular shape. However, provided this distortion is not great, there is near symmetry about the upper edge, and the addition of detector resolution effects would not be expected to produce a significant displacement of the apparent edge position (unlike the gamma case). Therefore, in the present work, the half-height of the top edge of the spectrum was accepted as a good measure of the true recoil edge position, care having been taken to disregard the multiple scattering component (indicated by a second, diffuse, edge at a lower light output than the single-scatter edge).

The proton light output deduced from the absolute neutron measurements is shown in Figure 18. The functional form chosen was a power law in proton energy, joining smoothly onto a straight line. (This combination is one of the functional forms available in NRESP7.)

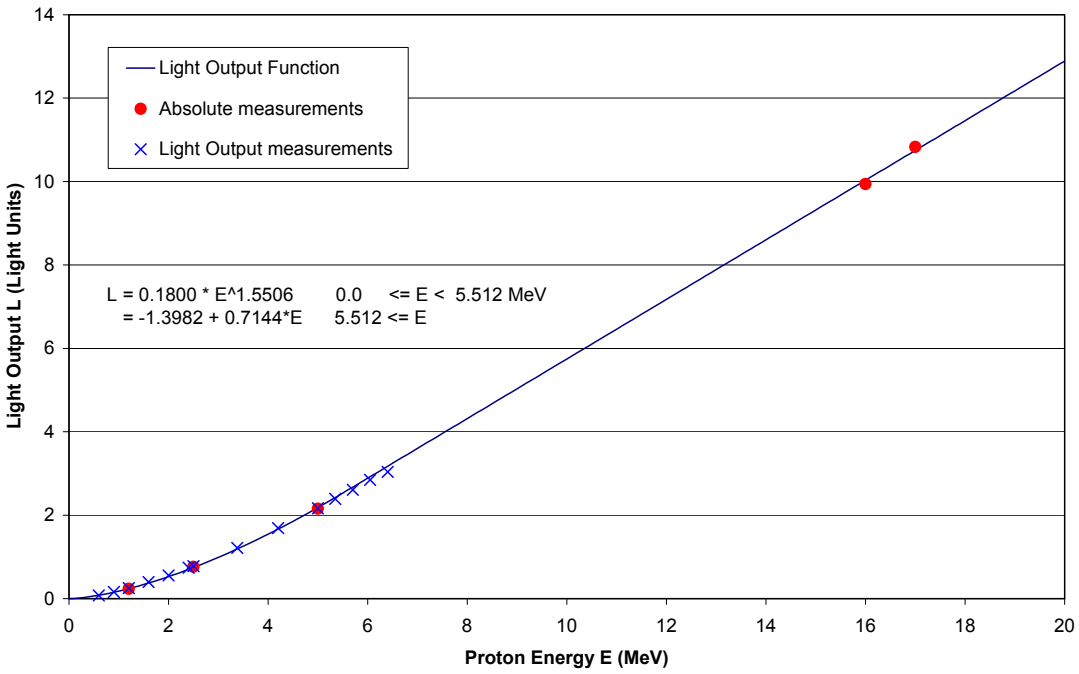

Figure 18. Proton light output for the Large spectrometer. The solid line is generated from the function shown, relating light output L in Light Units to proton energy E in MeV.

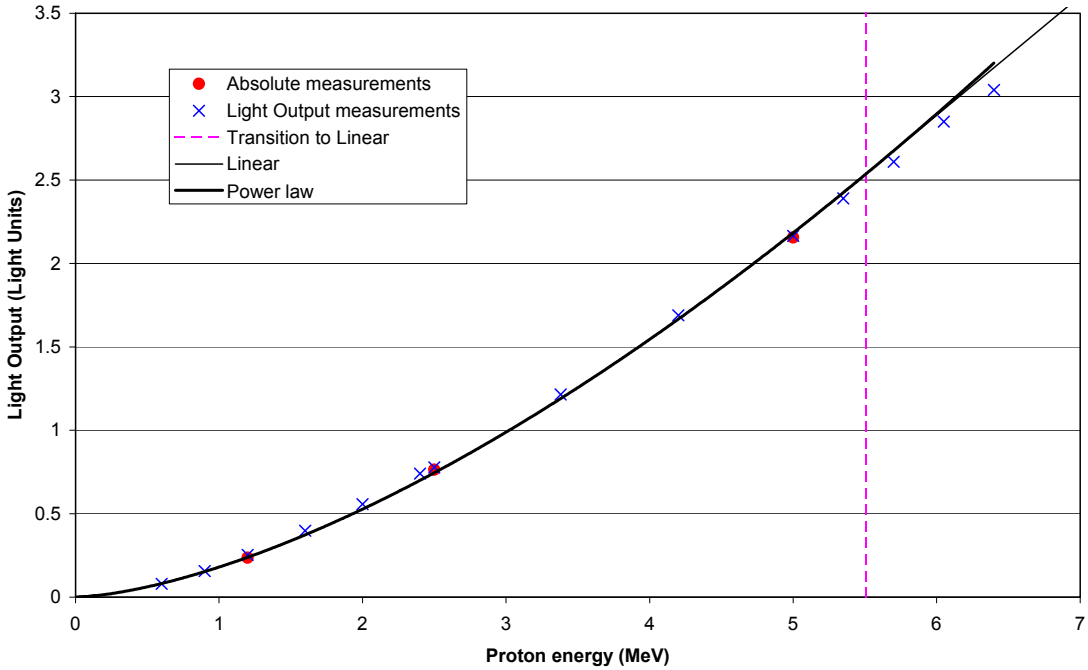

Figure 19. Low energy part of the proton light output for the Large spectrometer.

The low energy part of the function is shown separately in Figure 19. The purple dotted line shows the energy at which the transition from power law to linear fit is made.

The fit was initially carried out on the basis of the absolute neutron measurements alone (red dots), but this left large gaps in the energy coverage, so additional relative measurements of the light output were also made as described earlier (blue crosses). Below 5 MeV, the new measurements match the fit closely. There are signs of systematic deviation above 5 MeV, but it is difficult to change the parameters of the linear part because the high energy points at 16 and 17 MeV need to be included. No change was therefore made to the fit as a result of the additional measurements.

The variation of the underlying spectrometer resolution with light output was also deduced from the neutron data. This was done by measuring the 7/8 - 1/8 width of the recoil edge, and then applying a correction factor to convert this width to the FWHM of the underlying Gaussian smearing. In the case of fixed Gaussian smearing applied to a flat distribution with a perfectly sharp upper edge (step function), the FWHM is greater than the 7/8 - 1/8 width by a factor of 1.0235, and the same ratio was applied here. The results have already been shown in Figure 9, and, as pointed out then, the neutron data are seen to lie on the same curve as the gamma data.

Light output from ions other than protons is expected to be confined to low pulse heights. In the absence of data relating to the Large NE213 specifically, the default NRESP7 parameters were used.

5.2.2 Calculations of neutron pulse height spectra

The program NRESP7 could now be validated for this application by calculating pulse height spectra corresponding to the absolute neutron measurements described earlier.

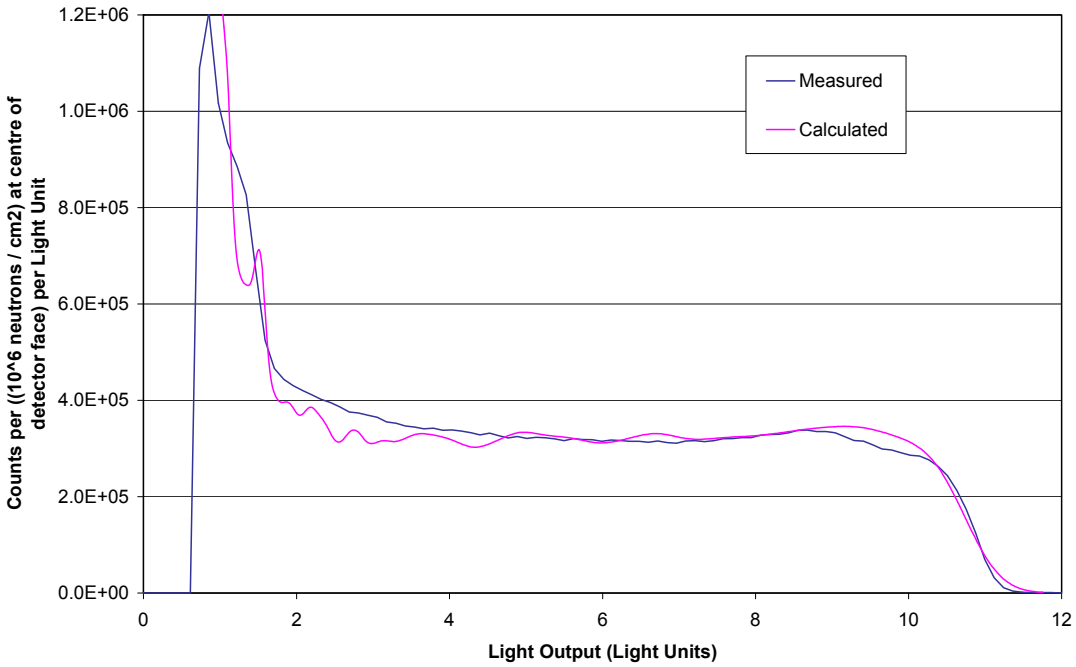

Figure 20. 17 MeV neutron pulse height spectrum, measured and calculated.

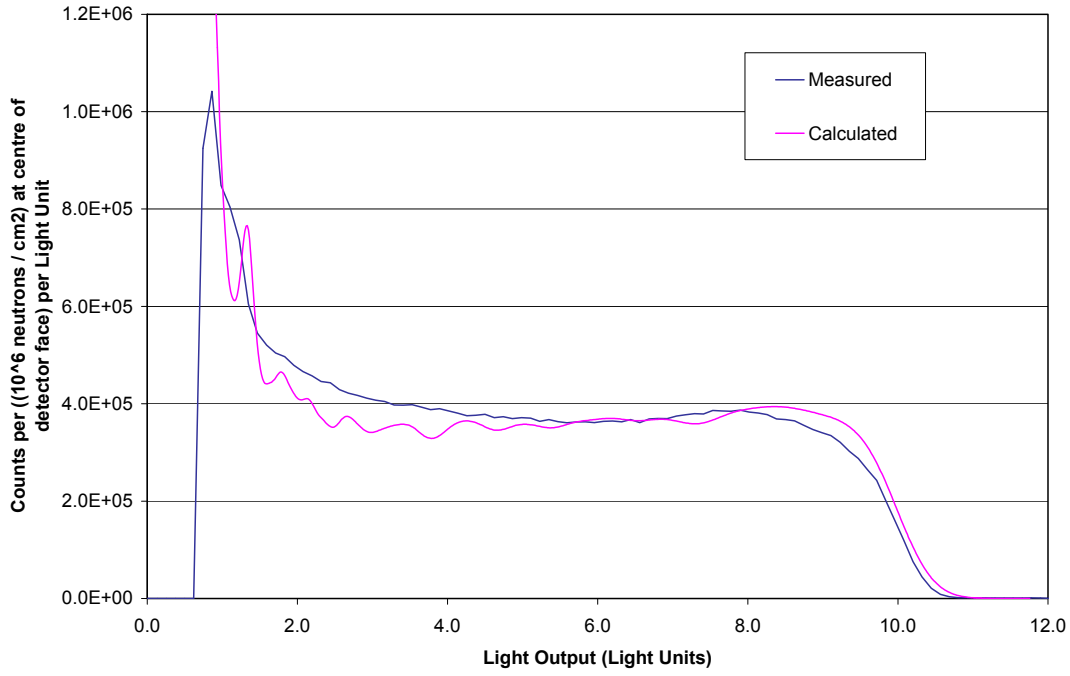

Figure 21. 16 MeV neutron pulse height spectrum, measured and calculated.

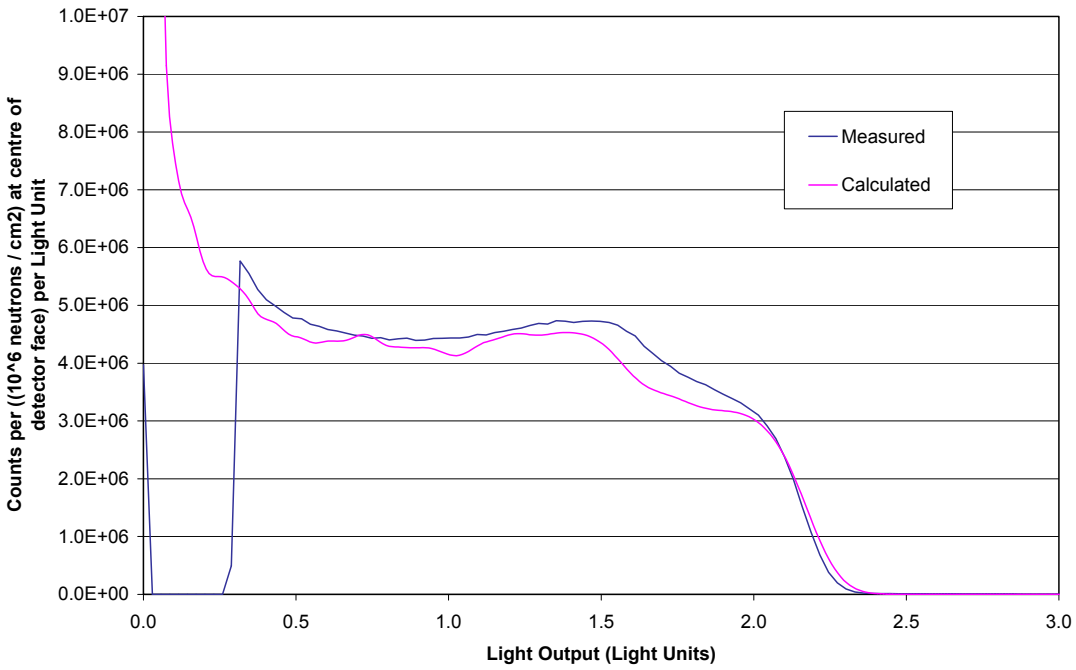

Figure 22. 5 MeV neutron spectrum, measured and calculated.

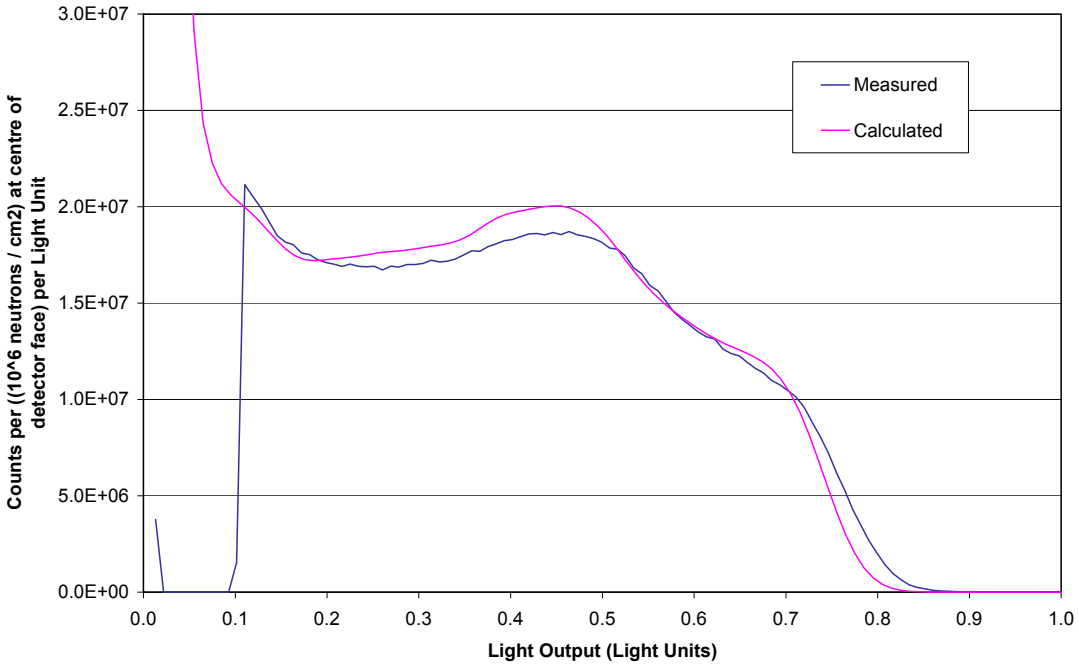

Figure 23. 2.5 MeV neutron pulse height spectrum, measured and calculated.

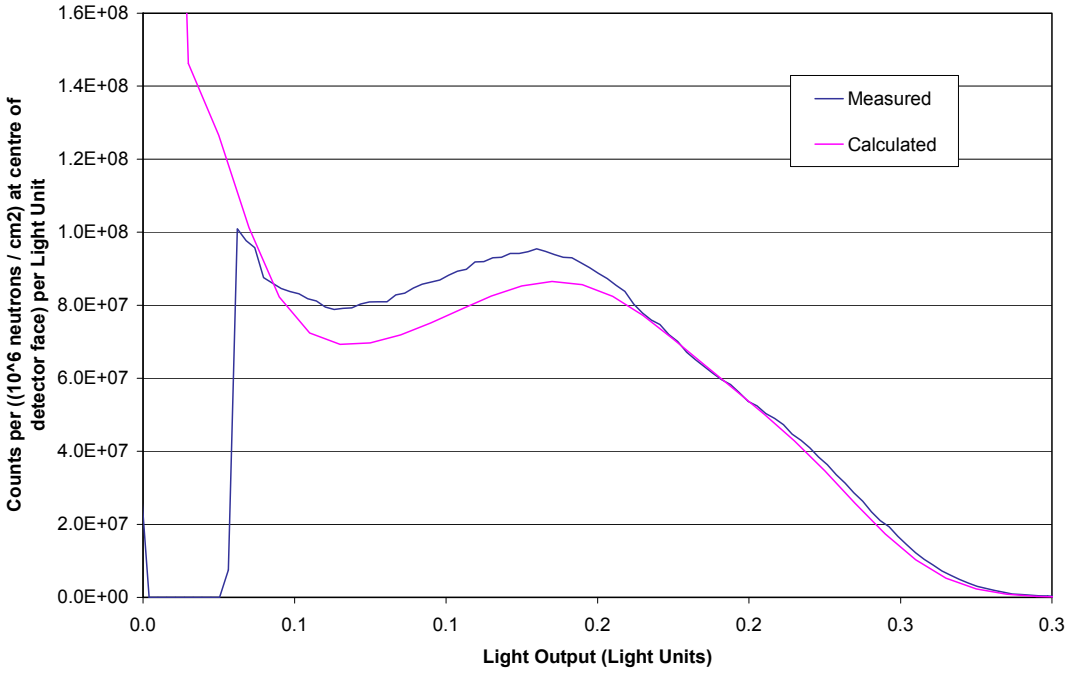

Figure 24. 1.2 MeV neutron pulse height spectrum, measured and calculated.

As with the gamma calculations, both horizontal and vertical scales are absolute, except in so far as the experimental spectrum contributed to the light output function. The match between measurement and calculation is again reasonable to good, especially at the higher neutron energies, and at the high light output end of the responses. In most cases of discrepancy, the measurement exceeds the calculation, as it did for gammas, and the explanation is presumably the same. There are, however, two places in the 16 and 17 MeV spectra where the calculation exceeds the measurement: at the upper end, where a small discrepancy might suggest a slight problem with the number and light output of multiple scattering events, and at about 1.5 light units, where a feature in the calculated spectrum fails to appear in the measurement.

5.2.3 Response matrix calculations

The neutron response matrix was assembled in a similar way to that for gammas. The NRESP7 calculation was set up for a distant (10 m) source as an approximation to a parallel beam, and the energies for the response calculations were again chosen so as to hold the number of response functions per resolution width ΔL approximately constant (at 3 this time). 115 response functions were calculated, at energies from 0.438 MeV to 12.135 MeV, with intervals varying from 52.3 keV to 276.5 keV. Two utility programs were written to help in the creation of the response matrix: one (in Visual Basic for Applications) to generate the large number of NRESP7 input lines needed to calculate all the responses, and another (in Fortran) to assemble those responses into a matrix in HEPROW format.

6 Simultaneous neutron and gamma measurements

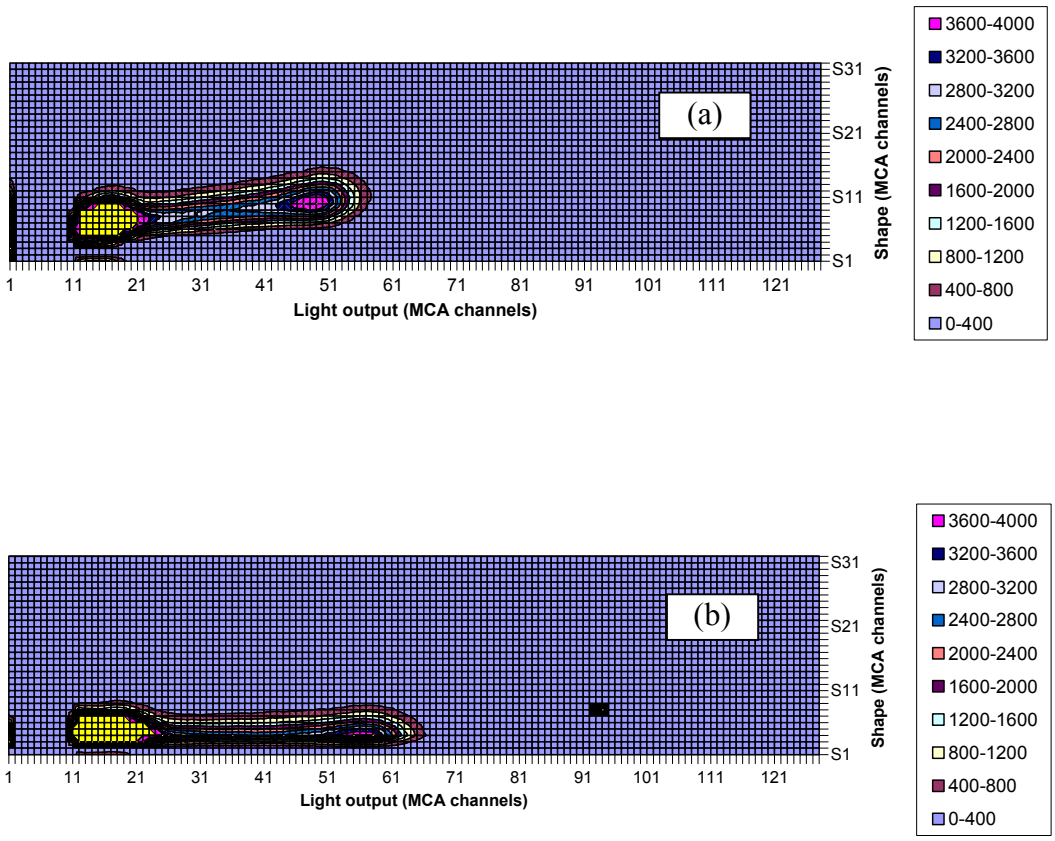

Figure 25. Multi-parameter acquisition of ^{22}Na spectrum.
(a) Data from June 2005; (b) Data from November 2005.
(The bright yellow colouration denotes cells with more than 4000 counts.)

One advantage of organic liquid scintillator spectrometers is the potential to acquire neutron and gamma spectra simultaneously. However, a problem has recently become apparent with the NPL system. Figure 25 shows two ^{22}Na spectra acquired in the usual dual-parameter mode, the second spectrum acquired 5 months after the first (with identical settings of the electronics). There has been a distinct rotation of the gamma branch in the intervening period, and it now hugs the zero channel of the Shape parameter. This gives rise to a possible loss of counts, because of the following property of the NPL dual parameter acquisition system.

If both ADCs are triggered but the Shape ADC does not subsequently produce any data (because the input was below the low level discriminator, for example), the event is ignored. There is therefore a narrow window between the Shape ADC's trigger threshold (100 mV in the NPL ADCs) and low level discriminator (typically 500 mV) within which events are lost. This may also distort the spectrum if more events are lost at some Energy values than at others. Spectrum (b) in the Figure may be suffering from this because of the very small Shape values associated with the whole gamma branch.

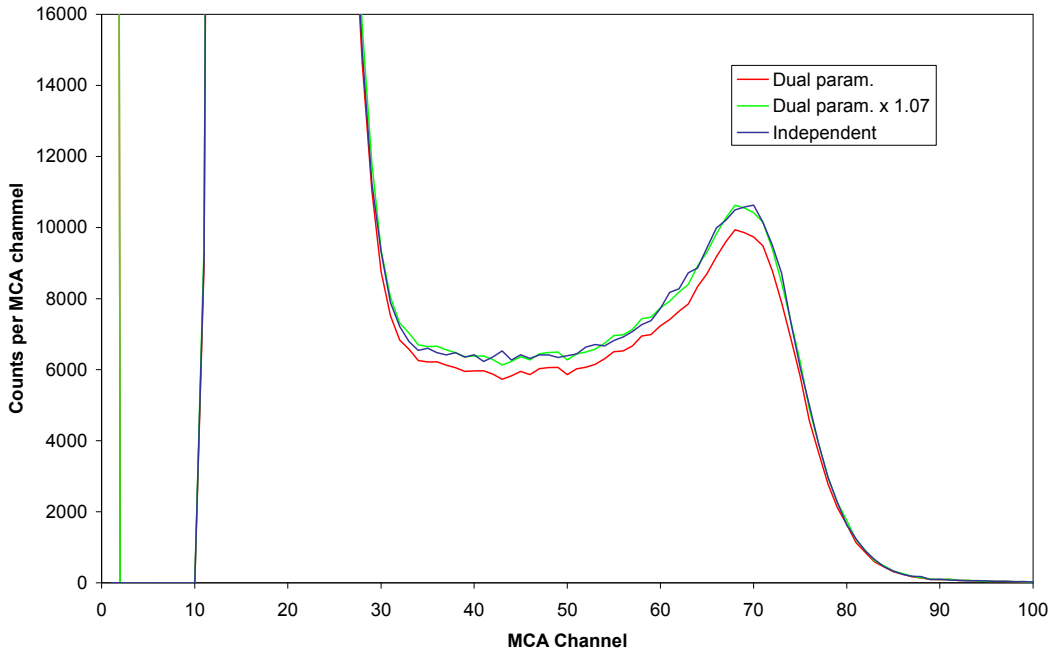

Figure 26. ^{22}Na data acquired in Dual Parameter and Independent modes.

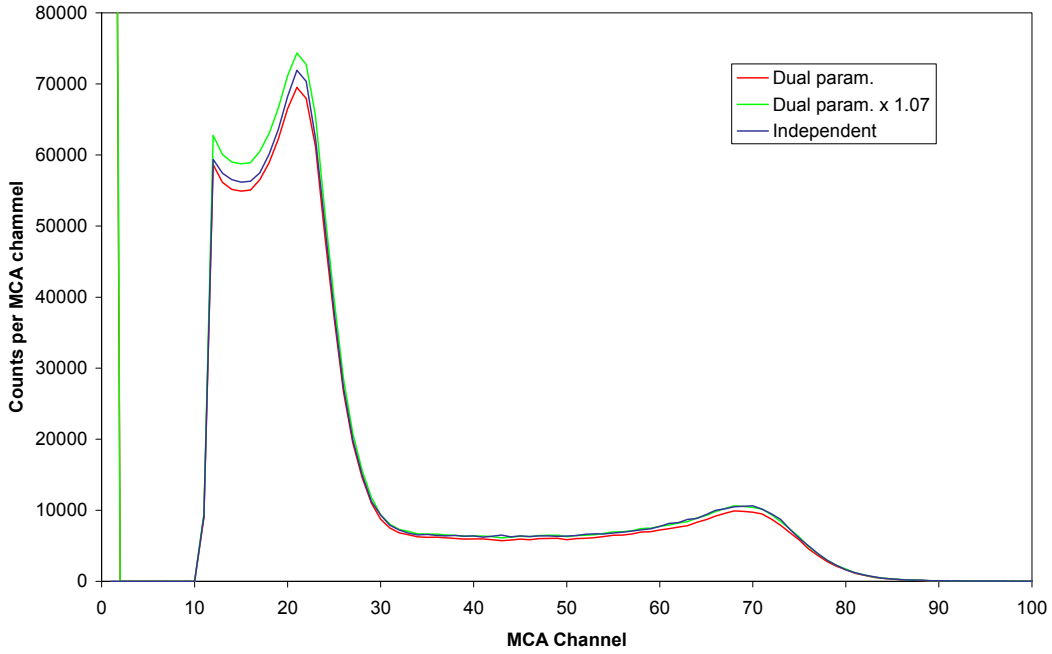

Figure 27. As above but with compressed vertical scale.

The reason for this rotation of the branch is not understood. Changing various electronic modules (pre-amplifier, main amplifier, ADC) produced no visible change. Possibly the effect arises from some interaction between the space charge saturation, which the Owen technique relies upon for discrimination, and a slow-acting alteration in the spectrometer characteristics, such as a gradual reduction under pressure of the amount of optical coupling compound between the optical components. It may be significant that the spectrum appears to have stretched to slightly higher amplitudes, as well as rotated, in the later measurement.

To prevent this problem from affecting the measured gamma spectra described earlier in this report, all the measurements were made in Independent mode, where the two ADCs are treated completely independently (i.e. as if the system consisted of two separate MCAs). This was possible because the gamma sources were known to be unaccompanied by neutrons.

An assessment of the scale of the problem was carried out by measuring a ^{22}Na gamma spectrum in the two modes, Dual Parameter and Independent, for the same number of seconds of live time (Figure 26 and Figure 27). It can be seen that there has been a loss of counts from the Dual Parameter spectrum over all channels. Multiplying the spectrum by 1.07 corrects this over a wide range of channels. At low pulse heights, however, this factor overcorrects to a small extent. This suggests that for the spectrum tested:

- In Dual Parameter mode the system was about 93% as efficient as it should have been over most of the pulse height range.
- At low pulse heights there is less loss of efficiency, implying a slight distortion of the spectrum shape.

The main advantage of the Owen technique is its avoidance of specialist electronics, but with the availability of powerful and inexpensive digital processing devices this may no longer weigh heavily. Instead the technique's disadvantages, namely its non-quantitative nature and the lack of control over it, are increasingly apparent.

7 Conclusions

The responses of the NPL liquid scintillation spectrometers to monoenergetic neutrons and gammas have been measured at various energies in the ranges 1.2 - 17 MeV approximately for neutrons and 0.28 - 1.8 MeV for gammas. The data for the Large spectrometer have been analysed to determine the proton light output function over the measured energy range, and also the resolution of the spectrometer as a function of light output.

The programs NRESP7 and PHRESP were used to calculate the neutron and gamma responses respectively of the Large spectrometer at the energies and geometries used in the measurements. Calculated and measured responses were compared, and found to be in reasonable to good agreement, particularly at the higher neutron and gamma energies and at the high light output end of the responses.

Using the same programs, neutron and gamma response matrices for the Large spectrometer were then generated in a format compatible with the unfolding program GRAVELW (part of the HEPROW suite). A pulse height spectrum from a ^{24}Na gamma source was measured and unfolded, and the positions of the peaks in the deduced energy spectrum were in good agreement with those expected.

An unexplained problem with the Owen technique for neutron / gamma discrimination means that gamma spectra measured in the presence of neutrons may suffer a small degree of distortion. Replacing the Owen system with digital electronics could solve this problem.

Analysis of the data measured with the Small spectrometer will be presented in a later report.

8 Acknowledgements

The authors are grateful to Ralf Nolte for his help with the measurements at PTB, and to Andy Bennett and Sarb Cheema for operating the NPL Van de Graaff accelerator. Thanks are also due to the NPL Radioactivity Group for their help with the ^{24}Na source, and to David Thomas for his helpful comments on the manuscript.

Financial support from the National Measurement System Programme Unit of the U.K. Department for Innovation, Universities and Skills is gratefully acknowledged.

Appendix: Stabilisation electronics

PTB has developed a stabilisation system for liquid scintillator spectrometers[16]. A light-emitting diode (LED) is incorporated into the scintillator cell, and is pulsed to produce standard flashes of light that are reproducible in terms of the number of photons per flash. A NIM-based control unit analyses the signals from the spectrometer and adjusts the high voltage to keep the response to the LED flashes constant. As LEDs are temperature sensitive, temperature compensation is included in the circuit that drives the LED so as to keep the standard flashes from changing with temperature. The system is designed to counter changes of temperature and count rate and the effects of storage or transport.

The NPL spectrometers do not include such stabilisation, and the question arises as to whether it should be included.

For work in the laboratory, the environmental parameters are well controlled. Temperature varies little, and in any case each measurement with the spectrometer is usually followed by a calibration with a reference source such as ^{22}Na. Count rates do vary, but are usually kept below about 10% dead time. For such measurements the added complexity of the stabilisation system appears to outweigh the benefits.

However, the spectrometers are also intended for use outside the laboratory, and here there is much less control of the environment. At the same time it is harder to ensure that a reference source is available for calibration. A system that maintained stability under changing conditions, especially one that dispensed with the need for a calibration check, would be a valuable asset.

In order to investigate the importance of the stability issue, rate tests were carried out with a ^{22}Na source positioned at three different distances on the axis of the Large NE213. Each measurement was run for the same number of seconds of live time. The results are shown in Figure 28 and Figure 29, in which the three spectra are normalised to the same integrated number of counts to that their shapes can be compared directly. The spectra are labelled with the total count rate in counts per second and the dead time in percent. There is a small but noticeable systematic increase in the position of the upper Compton edge with count rate, and a corresponding decrease in counts at the lowest pulse heights, possibly as a result of pulse pile-up. The effect is only minor, however, and one would normally try to avoid making measurements at the highest of the rates.

In conclusion, stabilisation does not seem necessary for laboratory measurements, but (if reliable) could be a real boon in the field. If new digital PSD electronics are developed for the spectrometers, the possibility of including a form of stabilisation at the same time should be considered.

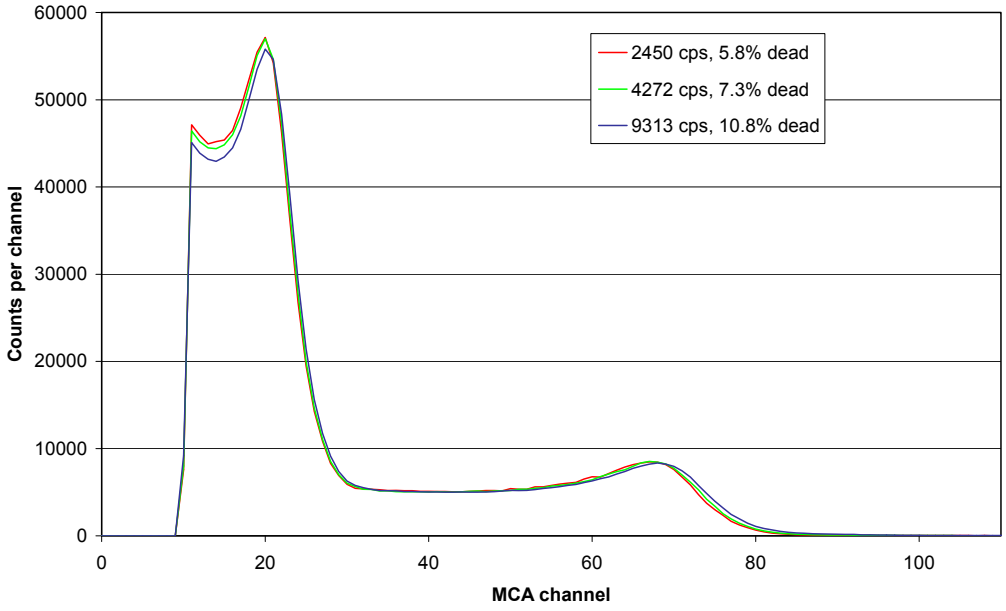

Figure 28. ^{22}Na spectra acquired at three different rates.

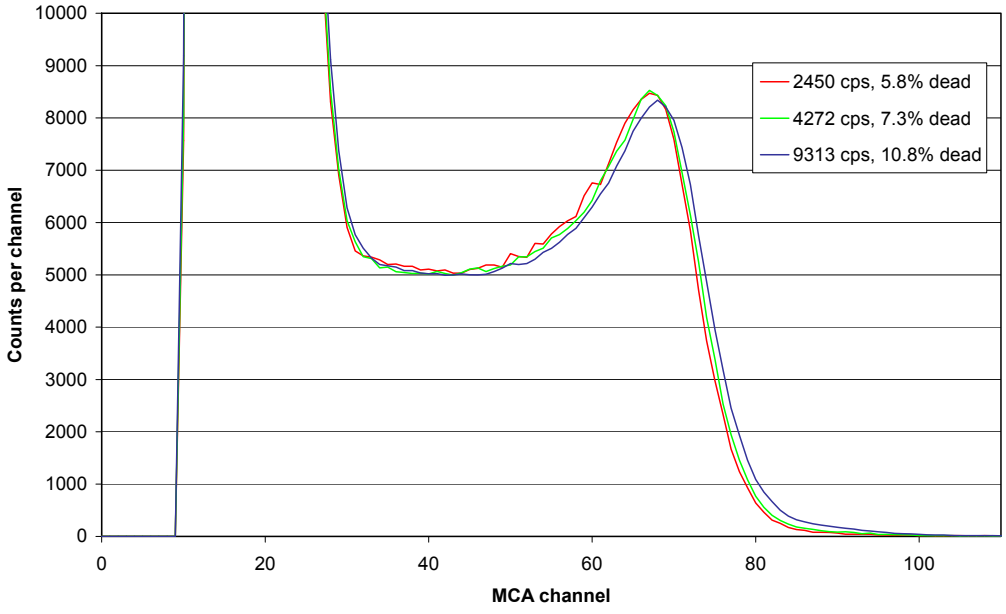

Figure 29. As previous Figure, but with an expanded vertical scale.

References

1. Saint-Gobain Crystals, www.detectors.saint-gobain.com
2. Stuart Green, Malcolm Scott and R. Koohi-Fayegh, *A users' guide for the NPL NE-213 Neutron Spectrometry System*, School of Physics and Space Research, University of Birmingham, September 1991, unpublished.
3. R.B. Owen, Nucleonics **17** No. 9 (1959) 92.
4. A.K. McCracken and M.J. Grimstone, *The experimental data processing program RADAK*, Proceedings of the First ASTM Symposium on Reactor Dosimetry, Petten, 1975.
5. R.E. Textor and V.V. Verbinski, *O5S: a Monte-Carlo code for calculating the pulse height distributions due to monoenergetic neutrons on organic scintillators*, Oak Ridge National Laboratory Report ORNL-4160 (1968).
6. J.M. Adams, N. Watkins, H. Klein and L. Lebreton, private communications, 2003 – 2004.
7. T. Novotny, *Photon spectrometry in mixed neutron-photon fields using NE213 liquid scintillation detectors*, PTB Report PTB-N-28, 1997.
8. G. Dietze and H. Klein, *NRESP4 and NEFF4: Monte Carlo codes for the calculation of neutron response functions and detection efficiencies for NE213 scintillation detectors*, PTB Report PTB-ND-22, October 1982 (with supplement for version 7, August 1991).
9. M. Matzke, Unfolding of pulse height spectra: the HEPRO program system, PTB Report PTB-N-19, 1994. (See also HEPROW.pdf, available from http://www.matzke-bs.de/heprow/heprow.htm.)
10. G. Dietze and H. Klein, *Gamma-calibration of NE213 scintillation counters*, Nucl. Instrum. Methods 193 (1982) 549 - 556.
11. T. Novotny, L. Büermann, S. Guldbakke and H. Klein, *Response of NE213 liquid scintillation detectors to high-energy photons (7 MeV < E_γ < 20 MeV)*, Nucl. Instrum. Methods in Phys. Res. **A 400** (1997) 356 - 366.
12. N.P. Hawkes, J.M. Adams, D.S. Bond, S. Croft, O.N. Jarvis and N. Watkins, *Measurements of the Proton Light Output Function of the Organic Liquid Scintillator NE213 in Several Detectors*, Nucl. Instrum. Methods in Phys. Res. **A 476** (2002) 190-194.
13. http://www.hightechsource.co.uk
14. http://www3.imperial.ac.uk/reactorcentre
15. G. Dietze, *Energy calibration of NE213 scintillation counters by γ-rays*, IEEE Transactions on Nuclear Science NS-26 (1979) 398 – 402.
16. K. Tittelmeier and H.-J. Barrenscheen, *Stabilisierung von Szintillationsdetektoren*, Laborbericht 6.42-03-2, PTB, September 2003.